7-2008

Nitrite Reduction by Siderite

Sudipta Rakshit
University of California, Berkeley

Christopher J. Matocha
University of Kentucky, cjmato2@uky.edu

Mark S. Coyne
University of Kentucky, mark.coyne@uky.edu

Nitrite Reduction by Siderite

Sudipta Rakshit
ESPM
Division of Ecosystem Sciences
140 Mulford Hall
Univ. of California
Berkeley, CA 94720

Christopher J. Matocha*
Mark S. Coyne
Dep. of Plant and Soil Sciences
Univ. of Kentucky
N-122R Agricultural Science Building-North
Lexington, KY 40546-0091

Nitrate-dependent Fe(II) oxidation is an important process in the inhibition of soil Fe(III) reduction, yet the mechanisms are poorly understood. One proposed pathway includes chemical reoxidation of mineral forms of Fe(II) such as siderite [$FeCO_{3(s)}$] by NO_2^-. Accordingly, the objective of this study was to investigate the reactivity of $FeCO_{3(s)}$ with NO_2^-. Stirred-batch reactions were performed in an anoxic chamber across a range of pH values (5.5, 6, 6.5, and 7.9), initial $FeCO_{3(s)}$ concentrations (5, 10, and 15 g L^{-1}) and initial NO_2^- concentrations (0.83–9.3 mmol L^{-1}) for kinetic and stoichiometric determinations. Solid-phase products were characterized using x-ray diffraction (XRD). Siderite abiotically reduced NO_2^- to N_2O. During the process, $FeCO_{3(s)}$ was oxidized to lepidocrocite [γ-$FeOOH_{(s)}$] based on the appearance of XRD peaks located at 0.624, 0.329, and 0.247 nm. The rate of NO_2^- reduction was first order in total NO_2^- concentration and $FeCO_{3(s)}$, with a second-order rate coefficient (k) of 0.55 ± 0.05 M^{-1} h^{-1} at pH 5.5 and 25°C. The reaction was proton assisted and k values increased threefold as pH decreased from 7.9 to 5.5. The influence of pH on NO_2^- reduction was rationalized in terms of the availability of $FeCO_{3(s)}$ surface sites (>$FeHCO_3^0$, >$FeOH_2^+$, and >CO_3Fe^+) and HNO_2 concentration. These findings indicate that if $FeCO_{3(s)}$ is present in an Fe(III)-reducing soil where fertilizer NO_3^- is applied, it can participate in secondary chemical reactions with NO_2^- and lead to an inhibition in Fe(III) reduction. This process is relevant in soil environments where NO_3^-– and Fe(III)-reducing zones overlap or across aerobic–anaerobic interfaces.

Abbreviations: XRD, x-ray diffraction.

Iron is the fourth most abundant element in mineral soils and is subject to changes in oxidation state (Essington, 2004). Microbial Fe(III) reduction to Fe(II) is an important process in anoxic soil environments because of its influence on organic C oxidation, soil physicochemical properties, and contaminant mobility (Lovley, 2000; Favre et al., 2002). During reduction of Fe(III) (oxy)hydroxides or phyllosilicate Fe(III), Fe(II) is released to solution and can undergo secondary processes such as adsorption and precipitation.

Siderite [$FeCO_{3(s)}$] is a common Fe(II) mineral produced as a result of secondary precipitation during microbial Fe(III) reduction under anoxic conditions (Coleman et al., 1993; Fredrickson et al., 1998; Zachara et al., 1998; Williams et al., 2005). Siderite has been shown to control Fe(II) solubility in anoxic sediments (Suess, 1979; Postma, 1982), rice paddy soil (Ratering and Schnell, 2000), subsoil peat horizons in close association with plant material (McMillan and Schwertmann, 1998), and coal overburden (Frisbee and Hossner, 1995; Haney et al.,2006). Oxidants for $FeCO_{3(s)}$ include O_2 (Frisbee and Hossner, 1995; Duckworth and Martin, 2004), Cr(VI) (Wilkin et al., 2005), H_2O_2 (Jambor et al., 2003), and $KMnO_4$ (Haney et al., 2006).

Nitrate inhibits Fe(III) reduction to Fe(II) in soils and sediments (Sorensen, 1982; Lovley, 2000). One explanation for this inhibition is NO_3^-–dependent Fe(II) oxidation, resulting in the anoxic production of Fe(III) (Lovley, 2000). Environments where NO_3^-–dependent Fe(II) oxidation is important include zones where NO_3^- reduction and Fe(III) reduction overlap (Weber et al., 2006). Concurrent NO_3^-– and Fe(III)-reducing zones have been reported in laboratory incubations of field soils and pure cultures (Komatsu et al., 1978; Obuekwe et al., 1981; DiChristina, 1992). Where concomitant NO_3^- and Fe(III) reduction occur, the biologically produced Fe(II) and NO_2^- can react chemically, producing Fe(III) and N_2O (Moraghan and Buresh, 1977). The Fe(III) product resulting from solution Fe(II) oxidation by NO_2^- was shown to be a poorly crystalline Fe(III) oxide mineral that was capable of affecting U cycling (Senko et al., 2005). The Fe(II)–NO_2^- chemical process has been invoked to explain the apparent inhibition of Fe(III) reduction in the presence of NO_3^- in pure cultures (Obuekwe et al., 1981) and anoxic paddy soil slurries (Komatsu et al., 1978). Cleemput and Baert (1983) showed that this reaction was more rapid as pH decreased. This may be attributed to the greater proportion of HNO_2 species. Protonation promotes N–O bond breaking, thus HNO_2 is a stronger oxidant than NO_2^- (Shriver et al., 1994). The presence of mineral surfaces such as Fe(III) (hydr) oxide minerals can readsorb Fe(II), leading to an acceleration in the electron transfer reaction rate to NO_2^- because surface Fe(II) is more reactive than dissolved Fe(II) (Sorensen and Thorling, 1991; Cooper et al., 2003).

Previously, NO_3^- was added to an agricultural surface soil under Fe(III)-reducing conditions and NO_3^-–dependent

Soil Sci. Soc. Am. J. 72:1070-1077
doi:10.2136/sssaj2007.0296
Received 10 Aug. 2007.
*Corresponding author (cjmato2@uky.edu).

Fe(II) oxidation occurred (Matocha and Coyne, 2007). It was suggested that this process was due in part to chemical reoxidation of mineral-associated Fe(II) by NO_2^-. One possible Fe(II) mineral that may have formed was $FeCO_{3(s)}$ based on thermodynamic modeling of soil filtrates; however, the role of $FeCO_{3(s)}$ in NO_2^- reduction is unclear. One could anticipate reduction of NO_2^- by $FeCO_{3(s)}$ because the redox couples for $FeCO_{3(s)}$ and oxidized Fe(III) minerals [such as lepidocrocite, γ-$FeOOH_{(s)}$] lie well below that of NO_2^-–N_2O (Fig. 1). This indicates that a thermodynamic driving force exists for the reaction to proceed. For $FeCO_{3(s)}$ to be important, one requirement is that it precipitate at relevant time scales. Siderite fulfills this requirement because precipitation is rapid, nearing completion within 4 h in the laboratory (Thornber and Nickel, 1976). Past studies have shown that mineral Fe(II) in wüstite [$FeO_{(s)}$] and green rust can readily reduce NO_2^- (Hansen et al., 1994; Rakshit et al., 2005) as well as Fe(II) bound on lepidocrocite (Sorensen and Thorling, 1991). Thus, the objective of this study was to investigate the reactivity of NO_2^- with siderite as a function of pH and reactant concentrations under anoxic conditions.

MATERIALS AND METHODS

Siderite Synthesis and Characterization

All the solutions were prepared using deionized water (18 Ω) that was made anoxic by purging with Ar for 3 h. To ensure anoxic environments, siderite synthesis and reactivity studies were conducted in an Ar–H_2 purged anaerobic chamber (Coy Laboratory Products, Grass Lake, MI). Siderite was synthesized by adding Na_2CO_3 to a stirred 0.5-L solution of $FeCl_2$ in equimolar amounts (0.5 mol L^{-1}) to form a pale gray precipitate, as described by Thamdrup et al. (1993). The siderite precipitate was washed with anoxic water to remove salts until the electrical conductivity of the wash water was lowered to background levels. The washed siderite was stored in suspension. The solid concentration of the siderite suspension was determined by weighing replicate subsamples. Subsamples of siderite were removed for characterization of alkalinity and solution Fe(II) at the native pH of the washed siderite (pH 8.0) and at pH 6.0. The pH and alkalinity values were used to calculate total carbonate concentration using MINEQL+ (Schecher and McAvoy, 1998), assuming a system closed to atmospheric CO_2. Solution Fe(II) was measured using the ferrozine [3-(2-pyridyl)-5,6 bis(4-phenylsulfonic acid)-1,2,4-triazine, monosodium salt] method by following absorbance at a wavelength of 562 nm (Stookey, 1970) with a ultraviolet–visible–near-infrared scanning spectrophotometer (Shimadzu, UV-3101 PC, Columbia, MD).

X-ray diffraction was used to characterize the gray precipitate. A slurry of the siderite mineral was mixed with Ar-degassed glycerol to prevent Fe(II) oxidation and dried under Ar. Scans were taken from 2 to 80° 2θ with CuKα radiation using a Siemens D-500 powder diffractometer fitted with a graphite monochromator and NaI (Tl) scintillation detector. The XRD peaks located at 0.359, 0.279, 0.234, 0.213, 0.196, 0.179, 0.173, 0.152, and 0.144 nm confirmed the presence of siderite (Sharp, 1960).

Stirred-Batch Experiments

Stock solutions of NO_2^- were prepared by dissolving certified ACS-grade $NaNO_2$ in deoxygenated, deionized water in a glove box. Reactions were performed in stirred-batch mode in duplicate 30-mL glass bottles. Experiments were initiated by adding aliquots of NO_2^- from the stock solution to the stirred siderite suspensions. In one set of experiments designed to evaluate the influence of initial $FeCO_{3(s)}$ concentration on the rate of NO_2^- reduction, $FeCO_{3(s)}$ was varied between 5 and 15 g $FeCO_{3(s)}$ L^{-1} [corresponding to Fe(II) concentrations of 0.04–0.12 mol L^{-1}], while NO_2^- concentration was held constant (4.6 mmol L^{-1}) at pH 5.5. In another set of experiments, the initial NO_2^- was varied between 0.83 and 9.3 mmol L^{-1} at a constant $FeCO_{3(s)}$ concentration of 10 g L^{-1} at pH 5.5. In addition, the rate of NO_2^- reduction was followed at pH 6.0, 6.5, and 7.9. The biological buffers MES [2-(*N*-morpholino)ethane sulfonic acid], PIPES (1,4-piperazine diethane sulfonic acid), and HEPES [1-piperazineethane sulfonic acid, 4-(2-hydroxyethyl)-monosodium salt] with concentrations of 0.3 mol L^{-1} were added to control the pH (Alowitz and Scherer, 2002). The pH was monitored periodically and found constant throughout the experiment. All experiments were conducted at 25°C.

Blank experiments were performed [$FeCO_{3(s)}$ free] by shaking 4.6 mmol L^{-1} NO_2^- in MES at pH 5.5 to account for possible self-decomposition of NO_2^- (Cleemput and Baert, 1983). We performed another experiment in which 4.6 mmol L^{-1} NO_2^- was added to dissolved Fe(II) extracted from the dissolving $FeCO_{3(s)}$ mineral to determine if dissolved Fe(II) could be responsible for the reaction. This experiment is referred to as "dissolved Fe(II)." Suspensions were removed periodically and filtered through a 0.2-μm membrane filter (Fisher Scientific, Hampton, NH). Ferrozine was added to the filtrates to complex and quantify dissolved Fe(II). The residue on the filter paper was washed with anoxic water to remove any NO_2^- present and treated with 0.5 mol L^{-1} HCl to dissolve Fe(II) present in the solid phase. The moles of solid-phase Fe(II) reacted were determined by comparing the Fe(II) concentrations in the solution and solid phases of reacted samples with that of a control $FeCO_{3(s)}$ experiment (NO_2^- free).

Nitrite concentration was measured using a Metrohm 792 Basic ion chromatograph (Herisau, Switzerland) with a MetroSep A column and MetroSep RP guard disk holder. The eluent was a mixture of 3.2 mmol L^{-1} Na_2CO_3 and 1 mmol L^{-1} HCO_3^- with conductivity detection. The retention time for NO_2^- was 6 min. The indophenol-blue method (Ngo et al., 1982) was used to measure NH_4^+. In separate experiments, N_2O was measured in the head space of capped

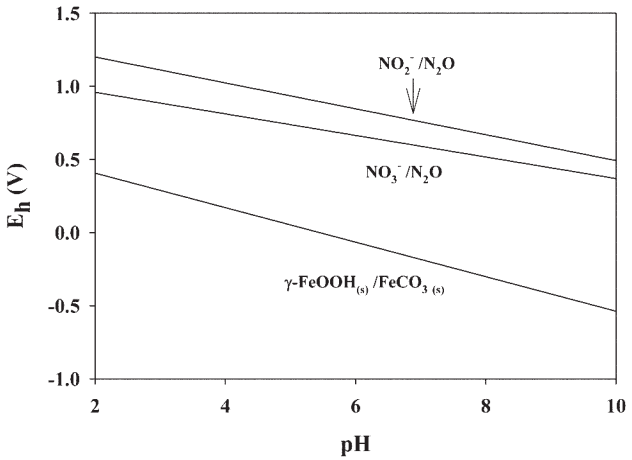

Fig. 1. A redox potential (E_h)–pH diagram for the N–Fe system. The concentration of solution NO_3^- and NO_2^- was taken to be 0.004 mol L^{-1}. The concentration of N_2O was 0.0003 mol L^{-1}. Standard reduction potentials (Eh^0) for the NO_2^-–N_2O and NO_3^-–N_2O couples were 1.396 and 1.116 V, respectively (Bard et al., 1985). The Eh^0 for the γ-$FeOOH_{(s)}$–$FeCO_{3(s)}$ couple was estimated from Gibbs free energy of formation values to be 0.86 V.

30-mL glass vials using a Varian 3700 gas chromatograph with a 2 mol L^{-1} packed column, Porapak Q, with a thermal conductivity detector and 20 mL min^{-1} He carrier gas.

Solid-phase reaction products were collected for samples reacted with 4.6 mmol L^{-1} NO_2^- for 24 and 96 h and compared with a control siderite sample. Slurries were mixed with glycerol, dried, and XRD was performed as described above.

RESULTS AND DISCUSSION

Stoichiometry

Siderite readily reduced NO_2^- (Fig. 2A–2C). For example, approximately 60% of the initial NO_2^- was lost from solution after 23 h at pH 5.5 and initial NO_2^- and $FeCO_{3(s)}$ levels of 4.6 mmol L^{-1} and 10 g L^{-1} (Fig. 2A). No significant NO_2^- loss occurred in the blank experiments [$FeCO_{3(s)}$ free] at pH 5.5 during the same time frame. This rules out self-decomposition of NO_2^-. Past studies have shown self-decomposition of NO_2^- to be important at pH < 5.0 (Bartlett, 1981). The major product identified for NO_2^- reduction was N_2O based on gas chromatography. No NH_4^+ was detected. Wet chemical extractions of Fe(II) showed that 0.50 ± 0.25 mmol L^{-1} was oxidized and 0.24 ± 0.1 mmol L^{-1} of NO_2^- was reduced after 1 h of reaction time in experiments containing 10 g L^{-1} $FeCO_{3(s)}$ and 4.6 mmol L^{-1} NO_2^- (Fig. 2A). This indicates a 2:1 consumption of Fe(II) per mole of NO_2^- reduced and is consistent with the formation of N_2O as the major product of NO_2^- reduction. Similarly, Sorensen and Thorling (1991) found N_2O as the major product of NO_2^- reduction in the presence of Fe(II) bound to lepidocrocite. Hansen et al. (1994) reported production of N_2O during reduction of NO_2^- by green rust.

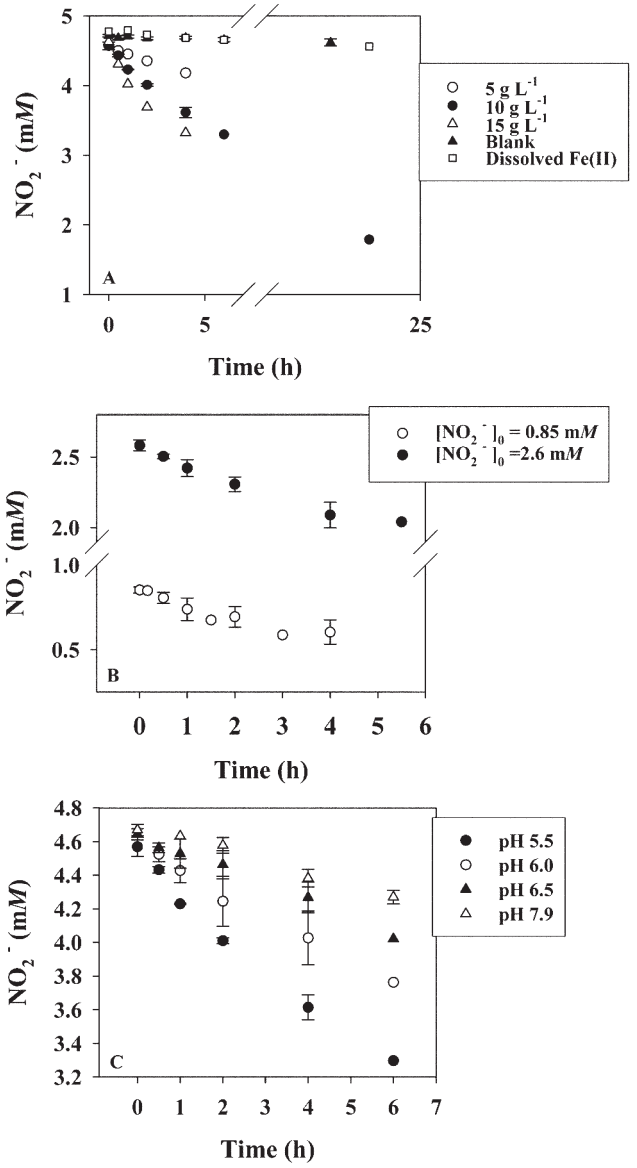

Fig. 2. Time course of NO_2^- reduction at (A) varying siderite level (5, 10, and 15 g L^{-1}) compared with a blank (siderite free) and dissolved Fe(II) sample with an initial NO_2^- concentration of 4.6 mmol L^{-1} at pH 5.5; (B) varying initial NO_2^- concentration at pH 5.5 and a siderite concentration of 10 g L^{-1}; and (C) varying pH values, with a siderite concentration of 10 g L^{-1} and NO_2^- of 4.6 mmol L^{-1}. Error bars represent the standard deviation from the mean for duplicate runs.

Solid-phase products were characterized using XRD in reacted and control (NO_2^- free) samples. The diagnostic d-spacings at 0.359, 0.279, 0.234, 0.213, 0.196, 0.179, 0.173, 0.152, and 0.144 nm revealed that $FeCO_{3(s)}$ was the sole mineral present after 96 h in control experiments (Fig. 3a). Siderite reacted with NO_2^- under identical conditions as in Fig. 2A [10 g L^{-1} $FeCO_{3(s)}$, 4.6 mmol L^{-1} NO_2^-, pH 5.5] showed a decrease in the intensity of the 104 reflection at 0.279 nm and the 116 reflection at 0.173 nm after 24 h of reaction (Fig. 3b), where approximately 2.8 mmol L^{-1} NO_2^- was reduced (Fig. 2A). At longer times (96 h) in the NO_2^-–reacted samples, the appearance of peaks at 0.624, 0.329, and 0.247 nm indicated the production of lepidocrocite [γ-$FeOOH_{(s)}$] (Fig. 3c). The weak feature at 0.173 nm could represent unreacted siderite or the 151 reflection of lepidocrocite. In addition to the lepidocrocite peaks, one diffraction peak was observed for goethite [α-$FeOOH_{(s)}$] at 0.420 nm.

Past studies have documented the important role of O_2 in siderite oxidation. Resulting oxidation products include ferrihydrite (Duckworth and Martin, 2004), lepidocrocite, and goethite (Senkayi et al., 1986; Frisbee and Hossner, 1995; Haney et al., 2006). Our results show that NO_2^- can function as an oxidant of siderite under anoxic conditions and produce lepidocrocite as the primary mineral, which coexisted with goethite (Fig. 3c). Lepidocrocite is metastable with respect to goethite (Schwertmann and Taylor, 1972; Ishikawa et al., 2005). It appears that poorly crystalline ferrihydrite formed in our experiments as a precursor to lepidocrocite based on the broad feature from 15 to 40° 2θ after 24 h (Fig. 3b). These results suggest the following overall reaction to be operative under our experimental conditions:

$$4FeCO_3(s)+2NO_2+2H^++H_2O \longleftrightarrow 4\gamma\text{-}FeOOH(s)+N_2O(g)+4CO_2(g) \quad [1]$$

It is possible that a homogeneous reaction involving dissolved Fe(II) in equilibrium with the solid $FeCO_{3(s)}$ and NO_2^- could occur in addition to the heterogeneous reaction with $FeCO_{3(s)}$. We tested this possibility by reacting NO_2^- with dissolved Fe(II) extracted from the dissolving $FeCO_{3(s)}$ mineral, referred to as "dissolved Fe(II)" in Fig. 2A. There was negligible reactivity in the reaction of NO_2^- with dissolved Fe(II) from the $FeCO_{3(s)}$ mineral within a period of 23 h (Fig. 2A). This suggests that structural Fe(II) in $FeCO_{3(s)}$ or adsorbed Fe(II)–$FeCO_{3(s)}$ species are involved in reducing NO_2^-.

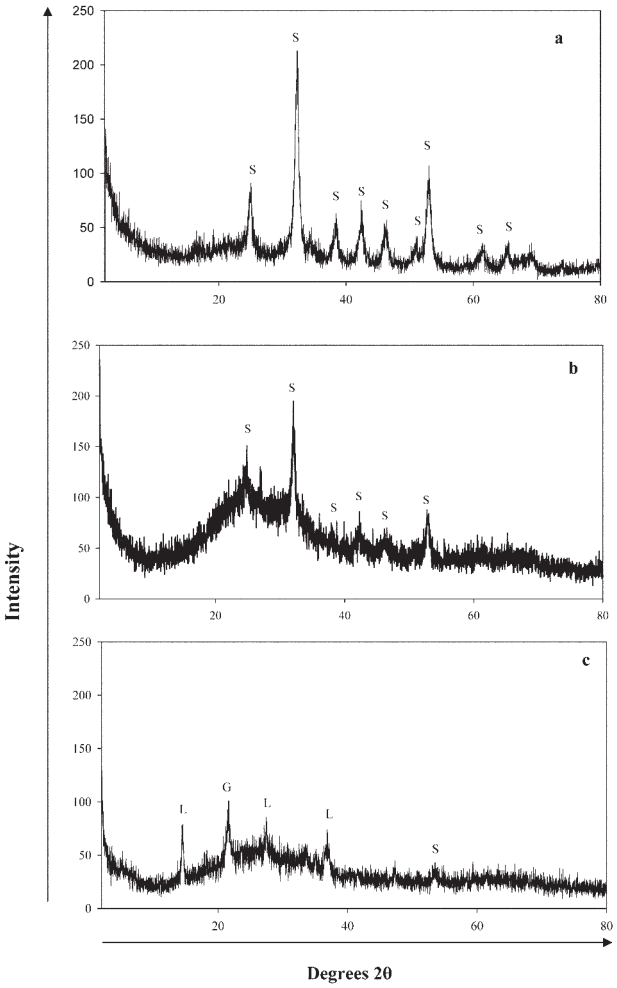

Fig. 3. X-ray diffraction patterns of the (a) control siderite after 96 h, (b) siderite reacted with 4.6 mmol L^{-1} NO_2^- after 24 h, and (c) siderite reacted with 4.6 mmol L^{-1} NO_2^- after 96 h. Experiments were performed at pH 5.5. S = siderite, L = lepidocrocite, and G = goethite.

Kinetic Analysis

Kinetic data were analyzed using the method of initial rates and isolation (Lasaga, 1981). One can write the overall rate equation for NO_2^- reduction by $FeCO_{3(s)}$ as

$$-\frac{d\left[NO_2^-\right]_T}{dt} = k\left[FeCO_{3(s)}\right]^x\left[NO_2^-\right]_T^y \qquad [2]$$

where $-(d[NO_2^-]_T/dt)$ is the rate of disappearance of $[NO_2^-]_T$, the sum of dissolved species of NO_2^-; k is the overall rate coefficient; and x and y are reaction orders for $FeCO_{3(s)}$ and NO_2^-, respectively. The initial reaction rate was determined by regression analysis of the initial linear phase of $[NO_2^-]_T$ removal. For experiments where an excess of NO_2^- is present at pH 5.5 and the initial concentration of NO_2^- is varied, Eq. [2] reduces to

$$-\frac{d\left[NO_2^-\right]_T}{dt} = k_I\left[NO_2^-\right]_T^y \qquad [3]$$

where $k_I = k[FeCO_{3(s)}]^x$. Taking the logarithm of both sides of Eq. [3] allows one to calculate y, the reaction order for NO_2^-, which is the slope of the least squares linear fit. In the same way, $[FeCO_{3(s)}]$ is varied at constant $[NO_2^-]_T$ and pH to calculate x.

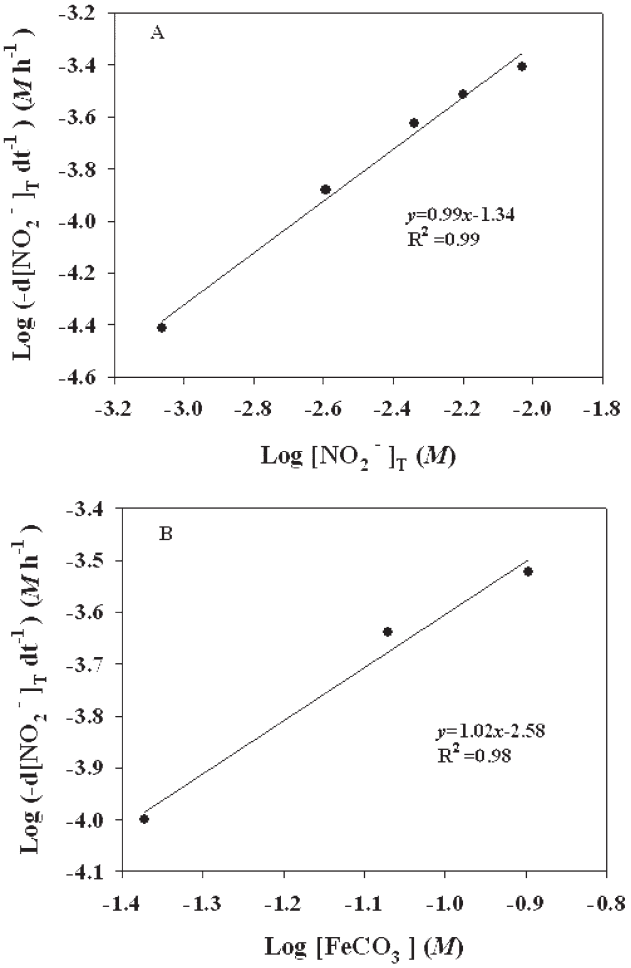

Fig. 4. Initial rate plots to determine apparent reaction order for (A) total NO_2^- concentration ($[NO_2^-]_T$) and (B) $FeCO_3$ concentration. The solid line represents a linear least square regression fit of the data.

There was a first-order dependence on $[NO_2^-]_T$ based on the slope of the regression, which is close to unity (Fig. 4A). These results differ from those of Hansen et al. (1994), where a zero-order dependence of NO_2^- was observed in the reduction by sulfate green rust. These differences may be explained by the differences in mineral structure. Sulfate green rust has a layered structure containing external and internal sites for NO_2^-, with SO_4^{2-} functioning as a charge-balancing interlayer anion (Hansen et al., 1994). Siderite, however, has a rhombohedral unit cell (Sharp, 1960) and possesses external reactive sites.

The reaction order for $[FeCO_{3(s)}]$ was 1.02 ± 0.02, which indicates a first-order dependence on $FeCO_{3(s)}$ (Fig. 4B). This implies a surface-controlled process and may be explained by the fact that at higher $FeCO_{3(s)}$ concentrations, more surface sites are available for reaction.

Thus, the reduction of NO_2^- by siderite can be described by an overall second-order rate expression:

$$\frac{-d\left[NO_2^-\right]_T}{dt} = k\left[FeCO_{3(s)}\right]^1\left[NO_2^-\right]_T^1 \qquad [4]$$

The average rate coefficient (k) calculated using Eq. [4] at pH 5.5 for the NO_2^- and siderite concentration ranges used (0.83–9.3 and 42–120 mmol L^{-1}, respectively) was 0.55 ± 0.05 M^{-1} h^{-1}.

The reduction of NO_2^- by siderite was pH dependent. The second-order rate coefficients increase threefold as pH

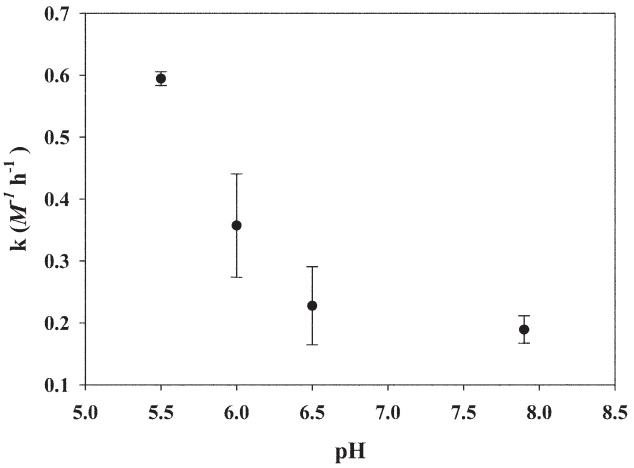

Fig. 5. Second-order rate coefficients for the reduction of NO_2^- by siderite at different pH values, for 10 g L^{-1} siderite and an initial NO_2^- concentration of 4.6 mmol L^{-1}.

decreased from 7.9 to 5.5 (Fig. 5). The influence of pH can be rationalized on the basis of the relative distribution of siderite surface sites and NO_2^- speciation.

Siderite bears several types of surface sites in the presence of water, based on comparisons from its isostructural counterpart, calcite (Van Cappellen et al., 1993). In the presence of water, siderite forms two primary sites on the surface, $>FeOH^0$ and $>CO_3H^0$ groups. The speciation of siderite surface sites has been described using the surface complexation model, where solution chemistry is related to surface complexes through equilibrium expressions (Van Cappellen et al., 1993; Pokrovsky and Schott, 2002). The $>FeOH^0$ and $>CO_3H^0$ groups on the siderite surface undergo protonation and deprotonation reactions and are characterized by stability constants (Table 1). The total number of reactive sites for $>FeOH^0$ groups, denoted as $[>Fe]_T$, is related to the sum of protonated and deprotonated surface species:

$$[>Fe]_T=[>FeOH^0]+[>FeO^-]+[>FeOH_2^+]+[>FeHCO_3^0]+[>FeCO_3^-] \quad [5]$$

One can rearrange and express Eq. [5] in terms of $[>FeOH^0]$:

$$\frac{[>FeOH^0]}{[Fe]_T}=\frac{1}{1+\frac{K_1}{[H^+]}+K_2[H^+]+K_3[H^+]^2[CO_3^{2-}]+K_4[H^+][CO_3^{2-}]} \quad [6]$$

where K_1 to K_4 correspond to the stability constants for Reactions 1 to 4 (Table 1). Expressions can be derived for $[>FeO^-]$, $[>FeOH_2^+]$, $[>FeHCO_3^0]$, and $[>FeCO_3^-]$ using Eq. [5] and [6] combined with their corresponding mass action equations. The concentration of CO_3^{2-} was calculated using MINEQL+ with the average of all alkalinity determinations, assuming a system closed with respect to atmospheric CO_2. We assumed a value for $[>Fe]_T$ of 4 $\times 10^{-4}$ mol sites L^{-1} based on crystallographic data as described by Wersin et al. (1989) under comparable experimental conditions [10 g $FeCO_{3(s)}$ L^{-1}]. Figure 6A shows the speciation of $>FeOH^0$ surface sites as a function of pH. Under our experimental conditions of pH 5.5 to 7.9, the $>FeHCO_3^0$ and $>FeOH_2^+$ sites are dominant fractions, followed by $>FeCO_3^-$ surface species (Fig. 6A). The $>FeOH^0$ and $>FeO^-$ species do not become important until much greater pH values, as observed elsewhere (Van Cappellen et al., 1993; Pokrovsky and Schott, 2002). A similar approach

Table 1. Surface complexation reactions and corresponding stability constants (*K*) considered in the siderite–water interface (temperature *T* = 298 K, ionic strength *I* = 0)†.

Reaction no.	Reaction	Log *K*
1	$>FeOH^0 \leftrightarrow >FeO^- + H^+$	−10.4
2	$>FeOH^0 + H^+ \leftrightarrow >FeOH_2^+$	10.2
3	$>FeOH^0 + CO_3^{2-} + 2H^+ \leftrightarrow >FeHCO_3^0 + H_2O$	22.75
4	$>FeOH^0 + CO_3^{2-} + H^+ \leftrightarrow >FeCO_3^- + H_2O$	14.65
5	$>CO_3H^0 \leftrightarrow >CO_3^- + H^+$	−4.4
6	$>CO_3H^0 + Fe^{2+} \leftrightarrow >CO_3Fe^+ + H^+$	−1.6

† Reactions from each site are located on the (104) plane (Pokrovsky and Schott, 2002).

was taken for the $>CO_3H^0$ surface sites using Reactions 5 and 6 (Table 1). Calculations for $>CO_3Fe^+$ were based on mean solution Fe(II) concentrations measured in control bottles at pH 6 and 7.9. Figure 6B shows that negatively charged species, $>CO_3^-$ sites, were predicted to be abundant, followed by $>CO_3Fe^+$ and $>CO_3H^0$.

The speciation of dissolved NO_2^- must be accounted for to help explain the pH dependence in its reduction rate. Total NO_2^- concentration ($[NO_2^-]_T$), which was measured in our experiments using ion chromatography, is the sum of protonated (HNO_2) and deprotonated (NO_2^-) forms and is expressed by the following mass balance expression:

$$[NO_2^-]_T=[HNO_2]+[NO_2^-] \quad [7]$$

Nitrite can undergo protonation and deprotonation reactions depending on pH:

$$HNO_2 \leftrightarrow NO_2^- + H^+ K_a = 5\times 10^{-4} \quad [8]$$

where K_a is the acid dissociation constant. Equations [7] and [8] can be rearranged to solve for $[HNO_2]$ and $[NO_2^-]$ as a function of pH:

$$[NO_2^-]_T=[HNO_2]\left(1+\frac{K_a}{[H^+]}\right) \quad [9]$$

There are several possible combinations of precursor surface complexes that may form in the transition state between siderite surface sites and different chemical species of NO_2^- to explain the pH dependence in Fig. 5. Of the $>FeOH^0$ surface sites, we assumed $>FeHCO_3^0$ and $>FeOH_2^+$ to be most important based on their abundance (see Fig. 6A). The $>CO_3Fe^+$ site, where Fe(II) is bound on $FeCO_{3(s)}$, was considered because past studies have shown that Fe(II) bound on lepidocrocite was reactive toward NO_2^- (Sorensen and Thorling, 1991). In addition, the possibility of $>CO_3Fe^+$ playing a role was suggested based on the lack of reaction between dissolved Fe(II) [in equilibrium with $FeCO_{3(s)}$] and NO_2^- (see Fig. 2A).

Possible precursor surface complexes were calculated as a product of their concentrations and as a function of pH (Fig. 7). This approach has been used elsewhere to describe sulfide oxidation by Fe(III) and Mn(IV) minerals and assumes that precursor surface complexation is rate limiting (Yao and Millero, 1993; Poulton, 2003). The products $[>FeHCO_3^0]$ $[HNO_2]$ and $[>CO_3Fe^+][HNO_2]$ sharply increased below pH

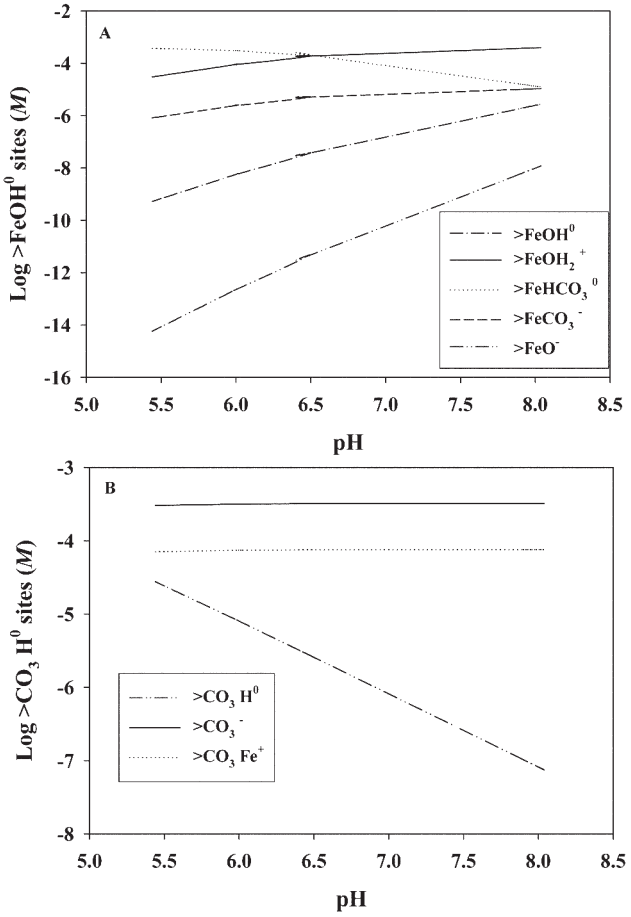

Fig. 6. The predicted surface speciation of (A) >FeOH^0 and (B) >CO$_3$H^0 sites of siderite. Equilibrium constants were taken from Table 1.

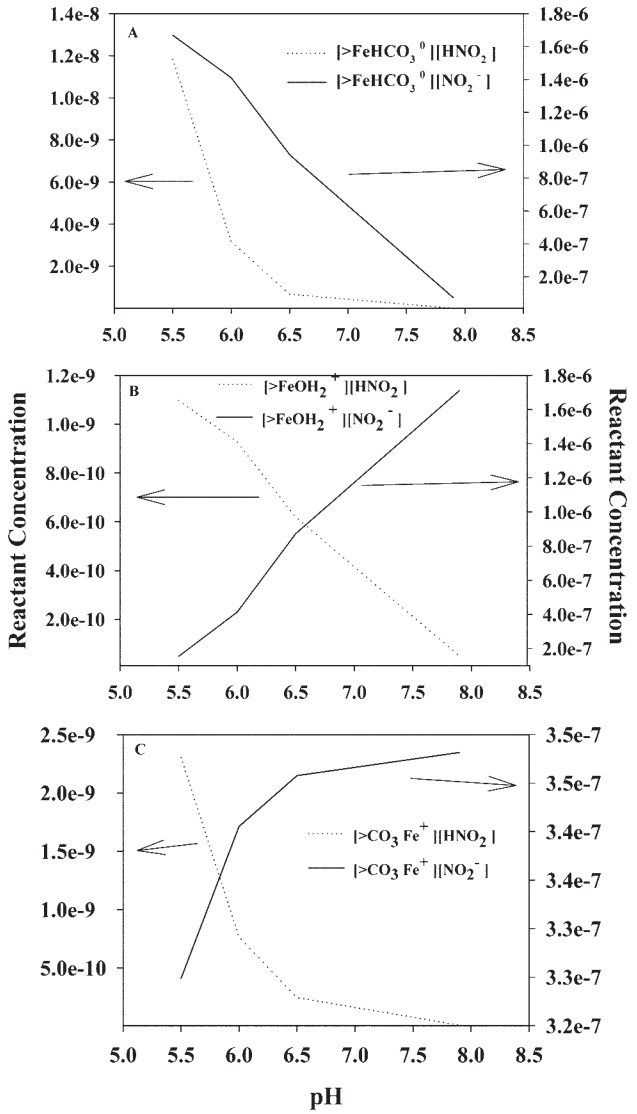

Fig. 7. Possible precursor surface complexes as a product of their concentrations and as a function of pH for (A) [>FeHCO$_3^0$][HNO$_2$] and [>FeHCO$_3^0$][NO$_2^-$]; (B) [>FeOH$_2^+$][HNO$_2$] and [>FeOH$_2^+$][NO$_2^-$]; and (C) [>CO$_3$Fe$^+$][HNO$_2$] and [>CO$_3$Fe$^+$][NO$_2^-$].

6.5 (Fig. 7A and 7C), which is similar to the trend in the reaction rate (Fig. 5). The [>FeHCO$_3^0$][NO$_2^-$] product increased with a decrease in pH as well and was in greater concentration than the other complexes (Fig. 7A, right-hand *y* axis).

The [>FeOH$_2^+$][HNO$_2$] form increased linearly with a decrease in pH (Fig. 7B). The Fe(II)–OH$_2$ bond is labile and would result in dissociation of H$_2$O. In solution chemistry, the water exchange rate for hexaaquo Fe(II) [Fe(H$_2$O)$_{6(aq)}^{2+}$] is rapid, estimated to be 3.2 ×10^6 s^{-1} (Shriver et al., 1994). The HNO$_2$ could bond directly to an exposed Fe(II) surface site and undergo electron transfer reactions. It is probable that the bonding mode of HNO$_2$ on Fe(II) is by the N atom, because this forms a stronger complex (Hitchman and Rowbottom, 1982; Shriver et al., 1994; Figgis and Hitchman, 2000). This configuration would allow the HNO$_2$ to serve as a π acceptor; thus, it would be able to accept electron density from the π system of Fe(II) (Luther et al., 1992).

The variations in [>FeOH$_2^+$][NO$_2^-$] and [>CO$_3$Fe$^+$][NO$_2^-$] are sensitive to pH, but in the opposite direction to the reaction rate (compare Fig. 5 with Fig. 7B and 7C). Therefore, they were ruled out as possible precursor surface complexes.

It is noteworthy that three out of the four possible precursor surface complexes ([>FeHCO$_3^0$][HNO$_2$], [>FeOH$_2^+$][HNO$_2$], and [>CO$_3$Fe$^+$][HNO$_2$]) involve HNO$_2$. Nitrous acid is a reactive oxidant toward Fe(II) species in solution. For example, oxidation of solution Fe(II) complexed with ethylenediaminetetraacetate exhibited a sharp increase in reaction rate with a decrease in pH. Kinetic modeling of the rate data revealed a second-order dependence on HNO$_2$ concentration (Zang et al., 1988). Protonation on the O weakens the N–O bond, allowing it to break (Shriver et al., 1994). Although [HNO$_2$] comprises only a small percentage of [NO$_2^-$]$_T$ even at the lowest experimental pH of 5.5 (∼0.7%), our data suggest that it is an important species kinetically.

Nitrite reduction by FeCO$_{3(s)}$ is a secondary reaction in the overall process of NO$_3^-$–dependent Fe(II) oxidation, a process relevant in environments where NO$_3^-$– and Fe(III)-reducing zones overlap or across aerobic–anaerobic interfaces. These environments could be present in poorly drained soils containing a shallow fragipan or in freshwater wetlands. Further experiments in our lab showed that NO$_3^-$ reactivity was negligible with FeCO$_{3(s)}$ for time periods up to 30 d (data not shown), despite the favorable thermodynamics (Fig. 1). Thus, where fertilizer NO$_3^-$ is added to soil under Fe(III)-reducing conditions [where FeCO$_{3(s)}$ controls Fe(II) solubility], it is probable that bacteria containing the nitrate

reductase enzyme would catalyze the first step of NO_3^- reduction to NO_2^- (Sorensen, 1982; Matocha and Coyne, 2007). Subsequently, $FeCO_{3(s)}$ would readily reduce NO_2^- to N_2O. Interestingly, NO_2^- was not detected as an intermediate in the overall process of NO_3^-–dependent Fe(II) oxidation in a field soil amended with NO_3^- (Matocha and Coyne, 2007). This could be due to rapid secondary chemical reduction of NO_2^- by $FeCO_{3(s)}$.

The abiotic production of N_2O during NO_2^- reduction by $FeCO_{3(s)}$ is significant because it is an important trace gas involved in global warming and depletion of the ozone layer (Galloway et al., 2003). There has been an increase in global N_2O emissions, with a significant part of the increase attributed to direct emissions from agricultural soils (Mosier et al., 1998). The rate expression derived from this study represents an important first step in modeling N_2O production in Fe(III)-reducing soil where fertilizer NO_3^- is applied and where $FeCO_{3(s)}$ controls Fe(II) solubility. The exact mechanism of NO_2^- reduction by $FeCO_{3(s)}$ remains to be established.

During the reduction of NO_2^-, $FeCO_{3(s)}$ is oxidized to γ-$FeOOH_{(s)}$. This is significant because it represents an anoxic pathway to mineral Fe(III) production and could impact the behavior of other nutrients such as phosphate, a well-known adsorbate to mineral Fe(III) surfaces (Essington, 2004). In addition, the anoxic production of γ-$FeOOH_{(s)}$ would contribute to the inhibition in Fe(III) reduction, a phenomenon that has been reported elsewhere (Obuekwe et al., 1981; Lovley, 2000).

CONCLUSIONS

The reduction of NO_2^- by siderite occurred readily. The main products of the reaction were N_2O and a solid Fe(III) mineral (lepidocrocite). The empirical rate expression was first order in each reactant. The second-order rate coefficients increased threefold as the pH decreased from 7.9 to 5.5. Although the second-order rate expression suggests that a bimolecular process is involved in the rate-limiting step, it is a composite expression and reflects the contribution of several possible combinations of siderite surface sites ($>FeHCO_3^0$, $>FeOH_2^+$, and $>CO_3Fe^+$) with reactive NO_2^- species ($[HNO_2]$). Additional experiments are needed to elucidate the structure of the activated complex between siderite surface sites and incoming NO_2^-. An example of an environment where this process may occur would be in overlapping NO_3^-– and Fe(III)-reducing zones where Fe(II) accumulates and reprecipitates as siderite and encounters NO_2^- produced from fertilizer NO_3^- applications.

ACKNOWLEDGMENTS

This project was supported by National Research Initiative Competitive Grant no. 2002-35107-12214 from the USDA Cooperative State Research, Education, and Extension Service.

REFERENCES

Alowitz, J.M., and M.M. Scherer. 2002. Kinetics of nitrate, nitrite, and Cr(VI) reduction by iron metal. Environ. Sci. Technol. 36:299–306.

Bard, A.J., R. Parsons, and J. Jordan. 1985. Standard potentials in aqueous solution. Marcel Dekker, New York.

Bartlett, R.J. 1981. Nonmicrobial nitrite-to-nitrate transformation in soils. Soil Sci. Soc. Am. J. 45:1054–1058.

Cleemput, O.V., and L. Baert. 1983. Nitrite stability influenced by iron compounds. Soil Biol. Biochem. 15:137–140.

Coleman, M.L., D.B. Hedrick, D.R. Lovely, D.C. White, and K. Pye. 1993. Reduction of Fe(II) in sediments by sulphate-reducing bacteria. Nature 361:436–438.

Cooper, D.C., F.W. Picardel, A. Schimmelmann, and A.J. Coby. 2003. Chemical and biological interactions during nitrate and goethite reduction by *Shewanella putrefaciens* 200. Appl. Environ. Microbiol. 69:3517–3525.

DiChristina, T.J. 1992. Effects of nitrate and nitrite on dissimilatory iron reduction by *Shewanella putrefaciens* 200. J. Bacteriol. 174:1891–1896.

Duckworth, O.W., and S.T. Martin. 2004. Role of molecular oxygen in the dissolution of siderite and rhodochrosite. Geochim. Cosmochim. Acta 68:607–621.

Essington, M.E. 2004. Soil and water chemistry: An integrative approach. CRC Press, Boca Raton, FL.

Favre, F., D. Tessier, M. Abdelmoula, J.M. Génin, W.P. Gates, and P. Boivin. 2002. Iron reduction and changes in cation exchange capacity in intermittently waterlogged soil. Eur. J. Soil Sci. 53:175–183.

Figgis, B.N., and M.A. Hitchman. 2000. Ligand field theory and its applications. Wiley-VCH, New York.

Fredrickson, J.K., J.M. Jachara, D.W. Kennedy, H. Dong, T.C. Onstott, N.W. Hinman, and S. Li. 1998. Biogenic iron mineralization accompanying the dissimilatory reduction of hydrous ferric oxide by groundwater bacterium. Geochim. Cosmochim. Acta 62:3239–3257.

Frisbee, N.M., and L.R. Hossner. 1995. Siderite weathering in acidic solutions under carbon dioxide, air, and oxygen. J. Environ. Qual. 24:856–860.

Galloway, J.N., J.D. Aber, J.W. Erisman, S.P. Seitzinger, R.W. Howarth, E.B. Cowling, and B.J. Cosby. 2003. The nitrogen cascade. Bioscience 53:341–356.

Haney, E.B., R.L. Haney, L.R. Hossner, and G.N. White. 2006. Neutralization potential determination of siderite ($FeCO_3$) using selected oxidants. J. Environ. Qual. 35:871–879.

Hansen, H.C.B., O.K. Borggaard, and J. Sørensen. 1994. Evaluation of the free energy of formation of Fe(II)–Fe(III) hydroxide–sulfate (green rust) and its reduction of nitrite. Geochim. Cosmochim. Acta 58:2599–2608.

Hitchman, M.A., and G.L. Rowbottom. 1982. Transition metal nitrite complexes. Coord. Chem. Rev. 42:55–132.

Ishikawa, T., K. Takeuchi, K. Kandori, and T. Nakayama. 2005. Transformation of γ-FeOOH to α-FeOOH in acidic solutions containing metal ions. Colloids Surf. A 266:155–159.

Jambor, J.L., J.E. Dutrizac, M. Raudsepp, and L.A. Groat. 2003. Effect of peroxide on neutralization-potential values of siderite and other carbonate minerals. J. Environ. Qual. 32:2373–2378.

Komatsu, Y., M. Takagi, and M. Yamaguchi. 1978. Participation of iron in denitrification in waterlogged soil. Soil Biol. Biochem. 10:21–26.

Lasaga, A.C. 1981. Rate laws of chemical reactions. Rev. Mineral. 8:1–68.

Lovley, D.R. 2000. Fe(III) and Mn(IV) reduction. p. 3–30. *In* D.R. Lovley (ed.) Environmental microbe–metal interactions. ASM Press, Washington, DC.

Luther, G.W., III, J.E. Kostka, T.M. Church, B. Sulzberger, and W. Stumm. 1992. Seasonal iron cycling in the salt marsh sedimentary environment: The importance of ligand complexes with Fe(II) and Fe(III) in the dissolution of Fe(III) minerals and pyrite, respectively. Mar. Chem. 40:81–103.

Matocha, C.J., and M.S. Coyne. 2007. Short-term response of soil iron to nitrate addition. Soil Sci. Soc. Am. J. 71:108–117.

McMillan, S.G., and U. Schwertmann. 1998. Morphological and genetic relations between siderite, calcite, and goethite in a Low Moor Peat from southern Germany. Eur. J. Soil Sci. 49:283–293.

Moraghan, J.T., and R.J. Buresh. 1977. Chemical reduction of nitrite and nitrous oxide by ferrous iron. Soil Sci. Soc. Am. J. 41:47–49.

Mosier, A.R., C. Kroeze, C. Nevison, O. Oenema, S. Seitziner, and O. Van Cleemput. 1998. Closing the global atmospheric N_2O budget: Nitrous oxide emissions through the agricultural nitrogen cycle. Nutr. Cycling Agroecosyst. 52:225–248.

Ngo, T.T., A.P.H. Pan, C.F. Yam, and H.M. Lenhoff. 1982. Interference in determination of ammonia with the hypochlorite–alkaline phenol method of Berthelot. Anal. Chem. 54:46–49.

Obuekwe, C.O., D.W.S. Westlake, and F.D. Cook. 1981. Effect of nitrate on reduction of ferric iron by a bacterium isolated from crude oil. Can. J. Microbiol. 27:692–697.

Pokrovsky, O.S., and J. Schott. 2002. Surface chemistry and dissolution kinetics of divalent metal carbonates. Environ. Sci. Technol. 36:426–432.

Postma, D. 1982. Pyrite and siderite formation in brackish and freshwater swamp sediments. Am. J. Sci. 282:1151–1183.
Poulton, S.W. 2003. Sulfide oxidation and iron dissolution kinetics during the reaction of dissolved sulfide with ferrihydrite. Chem. Geol. 202:79–94.
Rakshit, S., C.J. Matocha, and G.R. Haszler. 2005. Nitrate reduction in the presence of wüstite. J. Environ. Qual. 34:1286–1292.
Ratering, S., and S. Schnell. 2000. Localization of iron-reducing activity in paddy soil by profile studies. Biogeochemistry 48:341–365.
Schecher, W., and D.C. McAvoy. 1998. MINEQL+ Version 4.5. Environmental Research Software, Hallowell, ME.
Schwertmann, U., and R.M. Taylor. 1972. The transformation of lepidocrocite to goethite. Clays Clay Miner. 20:151–158.
Senkayi, A.L., J.B. Dixon, and L.R. Hossener. 1986. Todorokite, goethite, and hematite: Alteration product of siderite in East Texas lignite overburden. Soil Sci. 142:36–42.
Senko, J.M., Y. Mohamed, T. Dewers, and L.R. Krumholz. 2005. Role for Fe(III) minerals in nitrate-dependent microbial U(IV) oxidation. Environ. Sci. Technol. 39:2529–2536.
Sharp, W.E. 1960. The cell constants of artificial siderite. Am. Mineral. 45:241–243.
Shriver, D.F., P. Atkins, and C.H. Langford. 1994. Inorganic chemistry. 2nd ed. W.H. Freeman and Co., New York.
Sorensen, J. 1982. Reduction of ferric iron in anaerobic, marine sediment and interaction with reduction of nitrate and sulfate. Appl. Environ. Microbiol. 43:319–324.
Sorensen, J., and L. Thorling. 1991. Stimulation by lepidocrocite (γ-FeOOH) of Fe(II)-dependent nitrite reduction. Geochim. Cosmochim. Acta 55:1289–1294.
Stookey, L.L. 1970. Ferrozine: A new spectrometric reagent for iron. Anal. Chem. 42:779–781.
Suess, E. 1979. Mineral phases formed in anoxic sediments by microbial decomposition of organic matter. Geochim. Cosmochim. Acta 43:339–352.
Thamdrup, B., K. Finster, J.W. Hansen, and F. Bak. 1993. Bacterial disproportionation of elemental sulfur coupled to chemical reduction of iron or manganese. Appl. Environ. Microbiol. 59:101–108.
Thornber, M.R., and E.H. Nickel. 1976. Supergene alteration of sulphides: III. The composition of associated carbonates. Chem. Geol. 17:45–72.
Van Cappellen, P., L. Charlet, W. Stumm, and P. Wersin. 1993. A surface complexation model of the carbonate mineral–aqueous solution interface. Geochim. Cosmochim. Acta 57:3505–3518.
Weber, K.A., L.A. Achenbach, and J.D. Coates. 2006. Microorganisms pumping iron: Anaerobic microbial iron oxidation and reduction. Nat. Rev. Microbiol. 4:752–764.
Wersin, P., L. Charlet, R. Karthein, and W. Stumm. 1989. From adsorption to precipitation: Sorption of Mn^{2+} on $FeCO_{3(s)}$. Geochim. Cosmochim. Acta 53:2787–2796.
Wilkin, R.T., C. Su, R.G. Ford, and C.J. Paul. 2005. Chromium-removal processes during groundwater remediation by zerovalent iron permeable reactive barrier. Environ. Sci. Technol. 39:4599–4605.
Williams, A.G.B., K.B. Gregory, G.F. Parkin, and M.M. Sherer. 2005. Hexahydro-1,3,5-trinitro-1,3,5-triazine transformation by biologically reduced ferrihydrite: Evolution of Fe mineralogy, surface area, and reaction rates. Environ. Sci. Technol. 39:5183–5189.
Yao, W., and F.J. Millero. 1993. The rate of sulfide oxidation by δ-MnO_2 in seawater. Geochim. Cosmochim. Acta 57:3359–3365.
Zachara, J.M., J.K. Frederickson, S. Li, D.W. Kennedy, S.C. Smith, and P.L. Gassman. 1998. Bacterial reduction of crystalline Fe^{3+} oxides in single phase suspensions and subsurface materials. Am. Mineral. 83:1426–1443.
Zang, V., M. Kotowski, and R. van Eldik. 1988. Kinetics and mechanism of the formation of Fe^{II}(edta)NO in the system Fe^{II}(edta)/NO/HONO/NO_2^- in aqueous solutions. Inorg. Chem. 27:3279–3283.